Journal of Applied Polymer Science

Preparation and Characterization of Acrylic Acid/Itaconic Acid Hydrogel Coatings Containing Silver Nanoparticles

M. Guadalupe Rodríguez-Delgado,[1] Isaura G. Yáñez-Flores,[1] Saul Sánchez-Valdes,[1] Oliverio S. Rodriguez-Fernandez,[1] Rebecca Betancourt-Galindo,[1] Tomas Lozano-Ramirez,[2] Eduardo Ramirez-Vargas,[1] Hortencia Ortega-Ortiz[1]

[1]Centro de Investigación en Química Aplicada, Saltillo, Coahuila 25294, Mexico

[2]Instituto Tecnológico de Cd. Madero, Cd. Madero, Tamaulipas 89440, Mexico

Correspondence to: I. G. Yáñez-Flores (E-mail: isaura.yanez@ciqa.edu.mx) or S. Sánchez-Valdes (E-mail: saul.sanchez@ciqa.edu.mx)

ABSTRACT: Hydrogel silver nanocomposites have been used in applications with excellent antibacterial performance. Acrylic acid (AA)/itaconic acid (IA) hydrogels silver nanocomposites were prepared and applied as a coating on a textile substrate. Hydrogel matrices were synthesized first by the polymerization of an AA/IA aqueous (80/20 v/v) solution and mixed with 2-2-azobis(2-methylpropionamide) diclorohydrate and *N,N′*-methylene bisacrylamide until the hydrogel was formed. Silver nanoparticles were generated throughout the hydrogel networks with an *in situ* method via the incorporation of the silver ions and subsequent reduction with sodium borohydride. Cotton (C) and cotton/polyester (CP) textile fibers were then coated with these hydrogel silver nanocomposites. The influence of these nanocomposite hydrogels on the properties of the textile fiber were investigated by infrared spectroscopy (attenuated total reflectance), scanning electron microscopy, energy-dispersive X-ray spectroscopy, and antibacterial tests against *Pseudomona aeruginosa* and *Staphylococcus aureus*. The better conditions, in which no serious aggregation of the silver nanoparticles occurred, were determined. It was proven that the textiles coated with hydrogels containing nanosilver had an excellent antibacterial abilities. © 2013 Wiley Periodicals, Inc. J. Appl. Polym. Sci. 130: 2713–2721, 2013

KEYWORDS: gels; nanostructured polymers; textiles

Received 14 September 2012; accepted 7 April 2013; Published online 31 May 2013

DOI: 10.1002/app.39375

INTRODUCTION

A growing interest in textile materials with antimicrobial properties has stimulated continuous research, both in industry and in academia,[1–3] into the modification of existing fibers and the production of safety yarns for medical applications, such as coverings for skin wounds and burns. Despite major advances in burn wound management, infection remains the leading cause of morbidity in thermally injured patients, and the search for different treatments and new ideas continues. Among the different types of antimicrobial treatments used to improve the antimicrobial performance of fibers, there is the coating of the fibers with a wide diversity of antimicrobial agents, such as quinolates, phenols, cyanurates, ammonium, and other metal compounds.[4,5]

It is known that silver nanoparticles and silver ions show strong biocidal effects against a wide range of microorganisms, including *Escherichia coli* and *Staphylococcus epidermis* among others and against all types of bacteria that commonly develop on skin wounds.[6–9] Several processes for the synthesis of silver nanoparticles have been reported; these include chemical reduction,[10–12] UV photolysis,[13,14] γ irradiation,[15] steam deposition,[16,17] and laser ablation.[18] Chemical reduction has been the most extensively studied process.

Several kinds of silver-containing materials that can be used for wound dressings have been reported; these include silver sulfadiazine containing chitosan-based wound dressings,[19,20] silver complexes and nanocomposites, nanosilver/cellulose acetate composite fibers, and silver nylon dressings.[21,22] The principal function of a wound dressing besides its the antibiotic ability is to provide an optimal healing environment, which includes isolation from the external environment through coverage of the wound surface to prevent further contamination or infection and the maintenance of a moist environment next to the wound surface.[23]

The use of a hydrogel as a wound covering is especially favorable because the fluids in the wound, in general, do not dry. It has been documented that the water content in hydrogels allows them to offer an immediate cooling of the surface of the wound or burn and supports a reduction in temperature for a period of up to 6 h;[24] this provides a sensation of mitigation.

Table I. Final Silver Content as Measured by Atomic Absorption

Sample	$AgNO_3/NaBH_4$	Absorbance at a wavelength of 328.1 nm	Sample silver concentration (wt %)
0.02*M* CHAg	0.02M/0.015*M*	0.085	0.161
0.06*M* CHAg	0.06M/0.045*M*	0.018	0.517
0.1*M* CHAg	0.1M/0.075*M*	0.059	2.145
0.14*M* CHAg	0.14M/0.105*M*	0.138	4.957
0.2*M* CHAg	0.2M/0.15*M*	0.154	5.459
0.01*M* CPHAg	0.01M/0.0075*M*	0.037	0.067
0.02*M* CPHAg	0.02M/0.015*M*	0.126	0.246
0.06*M* CPHAg	0.06M/0.045*M*	0.022	0.673
0.1*M* CPHAg	0.1M/0.075*M*	0.090	3.031
0.14*M* CPHAg	0.14M/0.105*M*	0.203	7.321
0.2*M* CPHAg	0.2M/0.15*M*	0.291	10.354
1*M* CPHAg	1*M*/2*M*	0.155	7.066

Varsha[25] prepared a hydrogel of poly(*N*-isopropylacrylamide-*co*-sodium acrylate) with it as a rector for the production of silver nanoparticles. Dong et al.[26] used a PEO-PPO [poly(oxyethylene)-poly(oxypropylene)-poly(oxyethylene)] block copolymer to prepare colloidal silver hydrosols. Uygun et al.[27] obtained hydrogels with silver nanoparticles by the *in situ* reduction of silver nitrate ($AgNO_3$) with citrate as a stabilizing agent during the photo-induced copolymerization of acrylamide and *N,N′*-methylene bisacrylamide. Only few studies have been done on the *in situ* incorporation of silver nanoparticles in textile substrates with hydrogels. One of them was that reported by Gupta et al.,[6] in which the silver nanoparticles were synthesized by chemical reduction in a cotton (C) textile substrate grafted with poly(acryl amide-*co*-itaconic acid).

In this study, therefore, great attempts were made to establish a method for the incorporation and dispersion of silver nanoparticles into acrylic acid (AA)/itaconic acid (IA) hydrogels to be applied as a coating of a textile substrate with enhanced antimicrobial properties for wound dressings. Two types of textile substrates were used: one of 100 wt % C and other of 70/30 cotton/polyester (CP). The final properties of this wound dressing were characterized by Fourier transform infrared (FTIR) spectroscopy, scanning electron microscopy (SEM), and energy-dispersive X-ray spectroscopy (EDAX), and their antimicrobial activities against *Pseudomona aeruginosa* and *Staphylococcus aureus* are reported.

EXPERIMENTAL

Materials

AA and itaconic acid (IA) were supplied by Sigma Aldrich. $AgNO_3$, sodium borohydride, 2-2′-azobis(2-methylpropionamide) diclorohydrate, and *N,N′*-methylenbis(acrylamide) from Sigma Aldrich were analytical grade and were used without further purification. C (100 wt %) and CP (70/30 w/w) CP were used as textile substrates.

Sample Preparation

An AA/IA aqueous (80/20 w/w) solution (50 mL) was mixed with 2-2-azobis(2-methylpropionamide) diclorohydrate (0.4 wt %), and *N,N′*-methylene bisacrylamide (0.75 wt %) in a flask with a magnetic shaker immersed in a bath to maintain a temperature of 60°C until the hydrogel was formed. A textile substrate was immersed in the formed hydrogel with the desired $AgNO_3$ content, and then it was dried for 24 h at room temperature and mixed with cold $NaBH_4$ for 3 h to reduce the silver ions from Ag^+ to Ag^0. The textile sample was washed three times in deionized water and dried at 50°C. The molar contents of $AgNO_3/NaBH_4$ (M/M) used were 0.01/0.0075, 0.02/0.015, 0.06/0.045, 0.1/0.075, 0.14/0.105, 0.2/0.15, and 1/2. The corresponding designations for these samples are given in Table I.

Characterization Methods

The FTIR–attenuated total reflectance spectra were recorded on a Nicolet 550 Magna-IR spectrometer at a 4-cm^{-1} resolution with 100 scans. FTIR analysis was performed to obtain information about the functional groups on the samples. The silver content was estimated with an atomic absorption spectrophotometer (Varian Spectra AA-250 Plus). The morphology, size, and dispersion of the silver particles and their distribution on the hydrogel were determined and elemental analysis was performed with a JEOL JSM-7401F with an scanning transmission electron microscopy (STEM) modulus and a field emission gun at an accelerating voltage of 200 kV. Image-J software was used to determine the particle size distribution. The samples were gold–palladium coated for SEM analysis. The specific areas of the samples were microanalyzed by SEM/EDAX to detect the main elements on the sample surface. The X-ray diffraction (XRD) patterns of the products were obtained with a Siemens D-5000 with Cu Kα X-ray radiation.

The microbiological tests were performed for qualitative purposes in potato dextrose agar (PDA) medium and for quantitative purposes, according to ASTM E 2149-01. The microbiological tests were performed with nutritive agar as a culture medium against the next bacteria, *P. aeruginosa* (ATCC #13388) and *S. aureus* (ATCC #6538), which were supplied by American Type Culture Collection. These microorganisms were grown in a Petri dish with agar as a culture medium, and

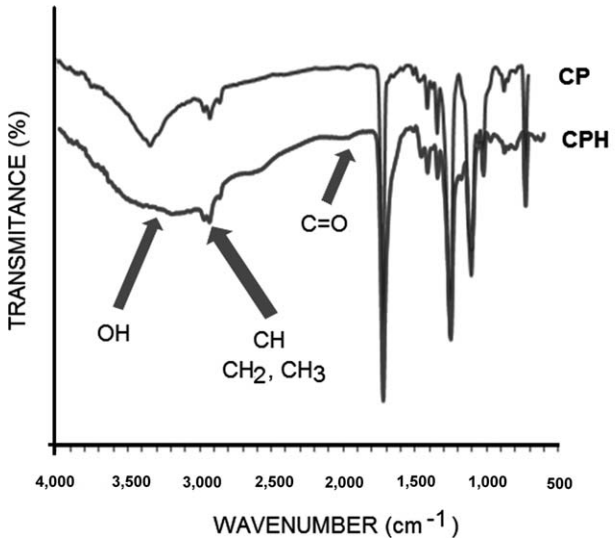

Figure 1. FTIR spectra of the CP and CPH substrates.

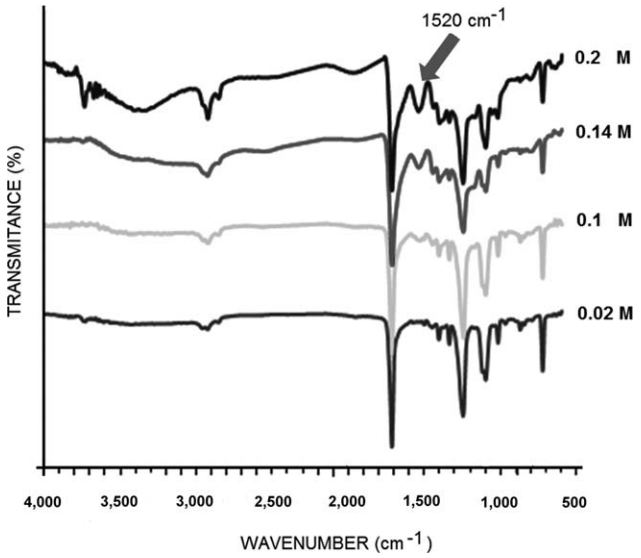

Figure 3. FTIR spectra of CPHAg.

then, the samples were located on the surface and were incubated for 48 h for the bacteria.

RESULTS AND DISCUSSION

FTIR Characterization

Figure 1 shows the FTIR spectra of the CP textile and the cotton/polyester textile with hydrogel (CPH) substrates. For the CP textile without hydrogel, a stretching band at 3340 cm^{-1} related to the OH groups was observed as well as the C-H stretching of methyl and methylenes at 2850–2950 cm^{-1} and the characteristic band at 1717 cm^{-1} of the C=O carbonyl groups from polyester in the CP textile fibers.[28,29] It was possible to detect the hydrogel in CPH by the stretching bands at 3340 and 2850–2950 cm^{-1}, which were related to the increase on the OH groups and the methyl and methylene groups associated with the hydrogel of the AA-*co*-IA copolymer.[28,30]

Figure 2 shows the characteristic bands of the C substrate at 3350 cm^{-1} associated with the OH groups and the bands at 2902–2914 cm^{-1} associated with the C-H of methyl and methylene groups. An additional stretching band at 1700 cm^{-1} was observed for the cotton with hydrogel substrate (CH) and was related to the C=O groups from the AA/IA copolymer of the hydrogel.

Figure 3 shows the infrared spectra of the cotton/polyester substrate coated with hydrogel and silver nanoparticles (CPHAg) at various molar contents of $AgNO_3$. The characteristic stretching bands of the CPH substrate were observed, particularly those representatives of the hydrogel at 3340 and at 2850–2950 cm^{-1} associated with the OH and CH groups of the hydrogel copolymer. There was a new band located at 1520 cm^{-1}; its intensity increased as the $AgNO_3$ concentration increased (0.1, 0.14, and 0.2*M*), and it has not been previously reported in the literature and could have been associated with the asymmetric and symmetric stretching of the N-O bonds.

In Figure 4, the FTIR spectra of the cotton substrate coated with hydrogel and silver nanoparticles (CHAg) is shown. In

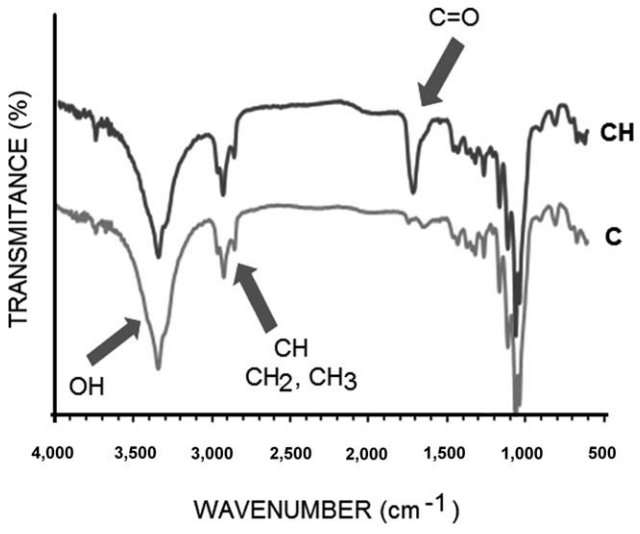

Figure 2. FTIR spectra of C and CH.

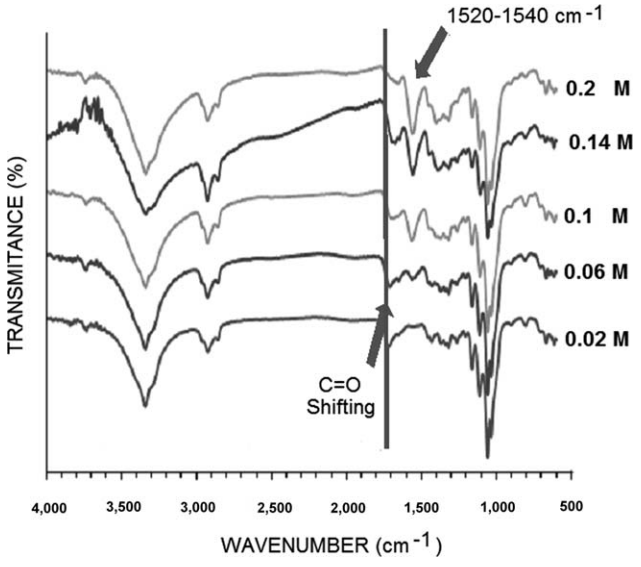

Figure 4. FTIR spectra of CHAg.

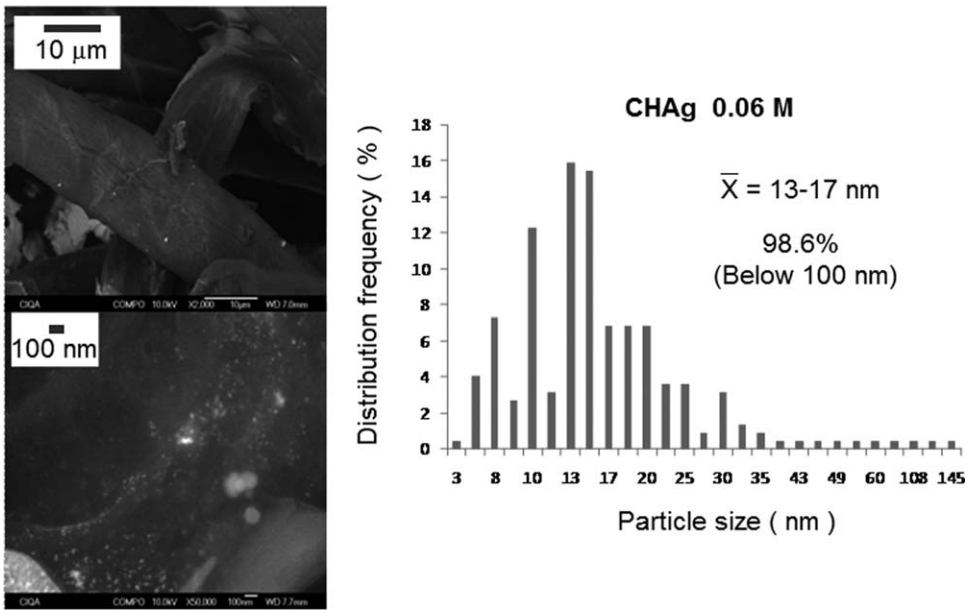

Figure 5. SEM images and histograms of silver particle distribution showing the average particle size $\bar{X}$ for the CHAg substrate with 0.06*M* $AgNO_3$.

addition to the characteristic stretching bands associated with the hydrogel described previously, shifts in the stretching band of the C=O group from 1700 cm^{-1} to 1691, 1662, 1653, 1639, and 1603 cm^{-1} for each of the $AgNO_3$ molar contents were observed. This indicated that as the silver salt was increased; the carbonyl band was shifted to lower wavelengths. This was in agreement with the results reported by Wen-Fu et al.,[31] who attributed this shift to the Ag-O bond. Nevertheless, in these spectra, it was also possible to observed the stretching band at 1520 to 1540 cm^{-1} for the 0.06, 0.1, 0.14, and 0.2*M* $AgNO_3$ concentrations, where we observed again an increase of the band transmittance as the concentration was increased.

When we compared Figures 3 and 4, higher intensity carbonyl bands (C=O) were observed for the CPH samples than for CH; this suggested that the CPH samples contained more hydrogel than the CH samples.

To determine the difference in hydrogel content in both types of substrates, coated and uncoated samples were weighed, and the results showed that the uncoated C samples weighed slightly more than the CP samples. A higher increase in weight was seen for the CPH-coated samples than for the CH-coated samples. This difference in hydrogel content between both substrates could have affected the final antimicrobial effect.

Atomic Absorption Spectroscopy

The final silver content in the textile samples after washing was determined by atomic absorption spectroscopy and is shown in Table I. The final silver content in the samples increased with increasing $AgNO_3$ molar concentration and reached a maximum level at 0.2*M*. When the molar ratio of 1*M*/2*M* $AgNO_3/NaBH_4$ was used, a reduction in the final silver content was observed; this suggested that an excess of $NaBH_4$ decreased the silver content and thus diminished the antimicrobial effect of the samples. This effect was also reported by Solomon et al.,[32] who found a noticeable reduction in their silver content when an excess of $NaBH_4$ was used.

SEM Characterization

SEM images and average silver particle distribution for the sample of the textile substrate of CHAg at 0.06*M* of $AgNO_3$ are shown in Figure 5. Textile C fibers coated with hydrogels could be seen in this image at lower magnifications. We observed white spots attributed to the silver particles and some silver particle aggregates. At higher magnifications, we observed good spherical silver particle dispersion and its distribution on the hydrogel that was coating the fiber. The particle size distribution obtained by the Image-J software indicated that most of the particle sizes were between 13 and 17 nm, whereas the rest of the particles were below 30 nm. This indicated that the *in situ* synthesis method was adequate for obtaining nanosilver particles.

Figure 6 shows the SEM images for CPHAg at 0.1*M* of $AgNO_3$. Good silver particle dispersion on the textile fiber with the hydrogel was observed. In the image at higher magnification, a good dispersion of silver nanoparticles on the substrate could be seen more clearly. The average particle size indicated that most of the silver particles were not higher than 30 nm, and the average particle size for this sample was between 8 and 15 nm. We also observed a few particle aggregates, but none higher than 100 nm, so these could be considered nanoparticles.

Figure 7 shows the SEM images for the CPHAg with an $AgNO_3$ content of 0.14*M*. Similar to the C substrate, the fibers of this sample showed good silver particle dispersion on the hydrogel coating, and a few particle aggregates could also be seen, although at higher magnifications, silver particles of different sizes were observed, with a few near 100 nm. This suggested that as the silver salt content was increased, an increase in the silver particle size also occurred. The silver particle size distribution

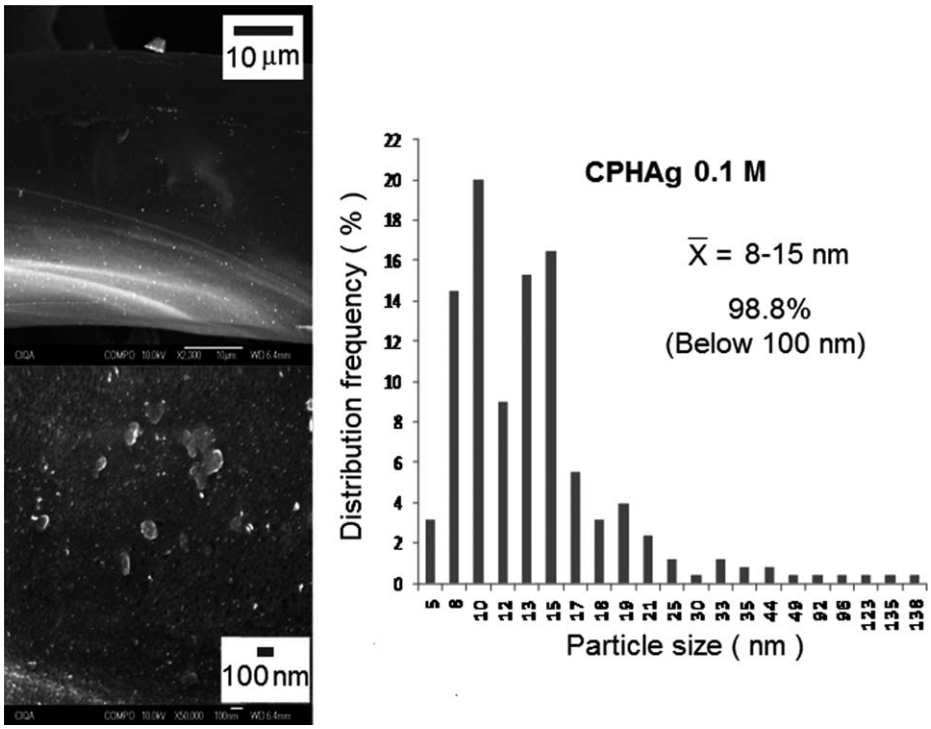

Figure 6. SEM images and histograms of silver particle distribution showing the average particle size $\bar{X}$ for the CPHAg substrate with 0.1*M* $AgNO_3$.

showed that most of the particles were between 61 and 91 nm; this was around 52% of the total particles, and these could be considered nanoparticles because they were under 100 nm.

In addition to the increase in the size of the silver particles, a higher tendency of the particles to form aggregates was observed as the molar content of the silver salt was increased. This was in agreement with results obtained by Lee et al.,[33] who reported an increase in the size of silver nanoparticles with increasing silver generator reactives; they also observed a tendency of the particles to form aggregates.

It was reported by Solomon et al.,[32] that an excess of $NaBH_4$ provided stability to the silver nanoparticles formed mainly

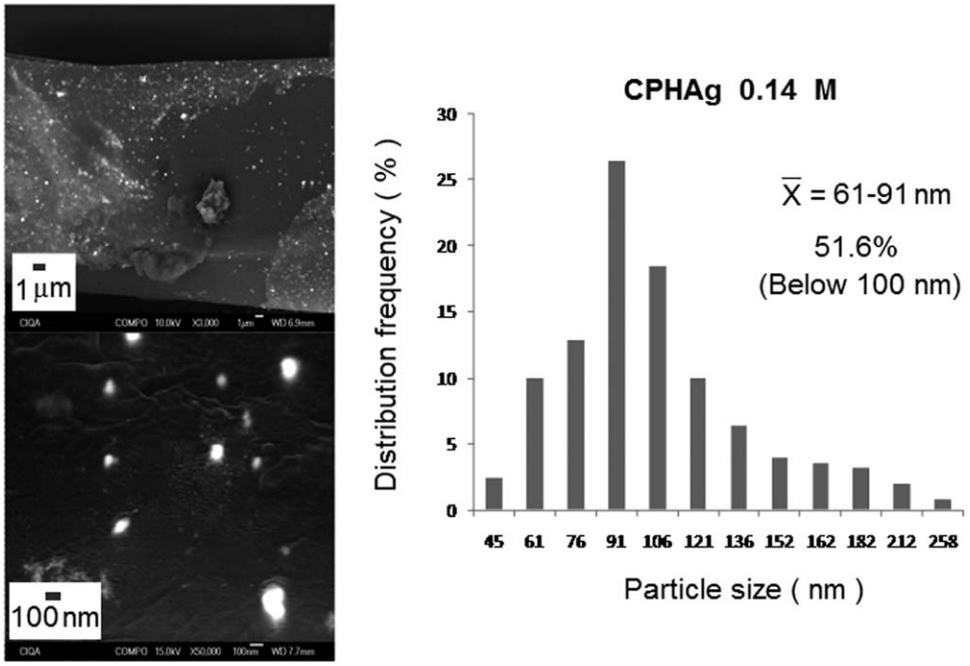

Figure 7. SEM images and histograms of silver particle distribution showing the average particle size $\bar{X}$ for the CPHAg substrate with 0.14*M* $AgNO_3$.

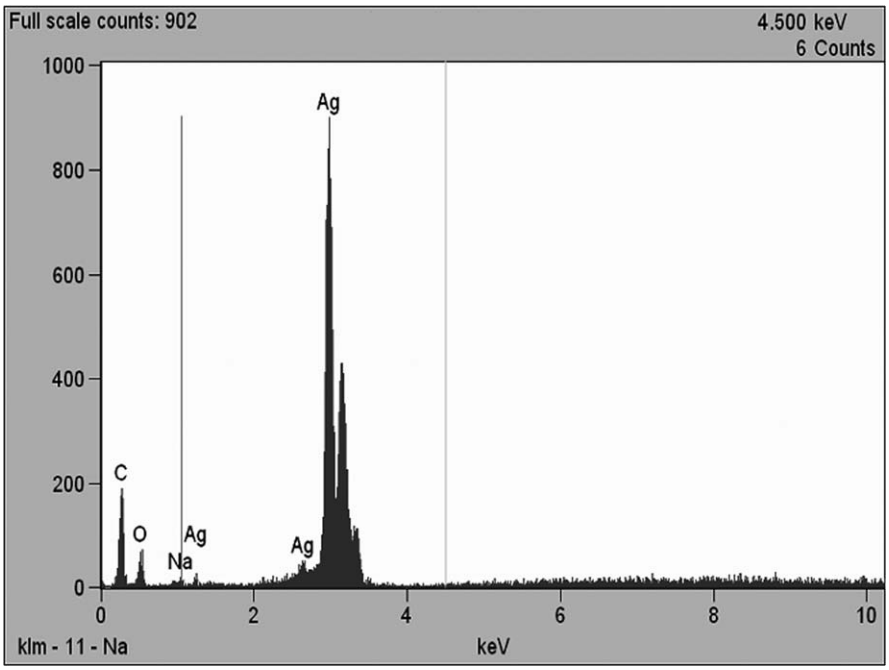

Figure 8. EDX analysis for the CPHAg substrate with 0.06*M* $AgNO_3$.

because of the repulsive forces of BH_4 around the particles that kept them separated. Nevertheless, after the reaction, too many $NaBH_4$ particles increased the ionic forces, which produced a global particle aggregation. This explained the observed particle aggregates and dispersed nanoparticles observed in samples with higher concentrations of $NaBH_4$.

EDAX

Figure 8 shows the elemental analysis for the sample of CPHAg with a 0.06*M* content of silver salt ($AgNO_3$). Carbon and oxygen were the main constituents of the textile substrate. Characteristic signals of silver were observed in this image, and this confirmed the presence of silver in this sample.

The sample CPHAg with a 0.1*M* content of silver salt is shown in Figure 9. It was possible to observe, in Figure 9(a), the hydrogel dispersed through the textile substrate and tiny particles on it. The scanning allowed the detection of silver in a large part of the sample, which appears as tiny spots in the micrograph in Figure 9(b); this showed the good dispersion of the silver nanoparticles on this substrate.

In this case, zones with higher contents of hydrogel were observed, and a higher concentration of silver in these zones was also observed. Because the hydrogel contained the silver ions to be reduced with $NaBH_4$ and was in the hydrogel where the silver nanoparticles[34] were formed, a higher hydrogel coating in the textile substrate led to a higher silver content.

XRD Characterization

The detection of the characteristic silver planes by XRD confirmed the presence of silver in the obtained samples. Figure 10(a) shows the XRD pattern for the sample with CP coated with hydrogel and with various silver contents. Characteristic diffraction peaks at 16 and 27° were observed, and these were attributed in other reports[35] to the CP substrate. On the other

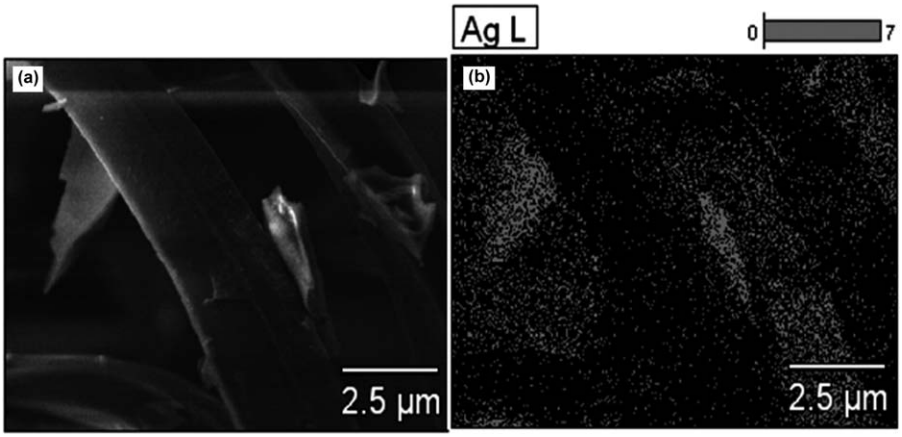

Figure 9. EDX images for the CPHAg substrate with 0.1*M* $AgNO_3$. AgL = Silver on the L energy level.

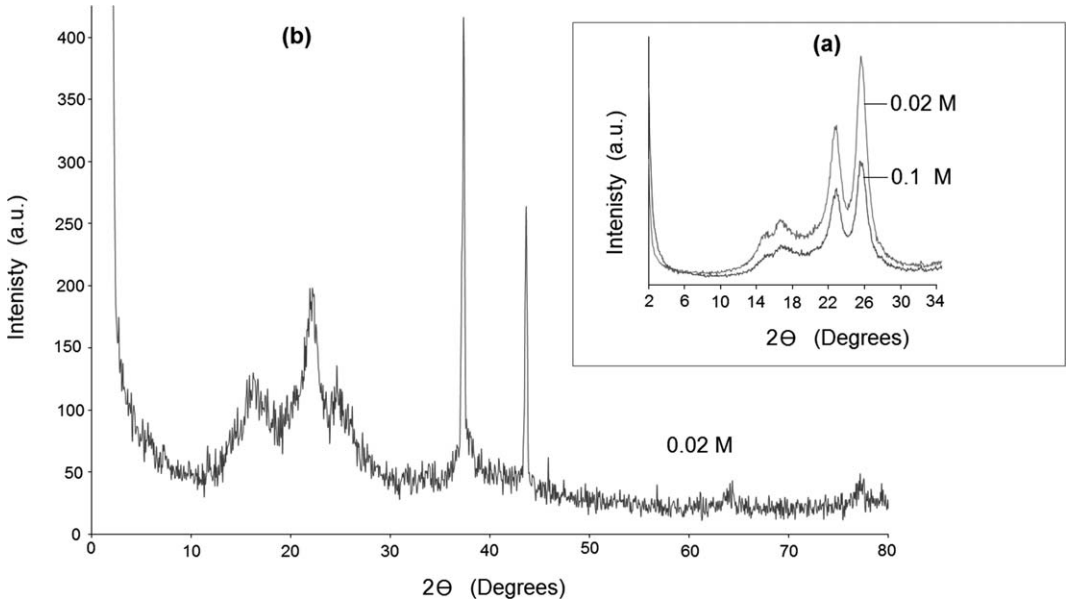

Figure 10. XRD scan for the CPHAg substrate with 0.02 and 0.1*M* $AgNO_3$: (a) from 2 to 34° and (b) from 0 to 80°.

hand, a characteristic diffraction peak at 38.1° was also observed; this was attributed to the characteristic silver 111 plane corresponding to of a face-centered cubic crystal. Commonly, this plane appears followed by the 200, 220, and 311 planes, which diffract at 44.2, 64.5, and 77.4°, respectively, which also correspond to the aforementioned crystalline structure of the silver[36,37] and which are also shown in Figure 10(b).

Antimicrobial Activity

To qualitative determine the antimicrobial effects of the obtained samples, images of the samples against *P. aeruginosa* and *S. aureus* were obtained. The results of antibacterial activity against *P. aeruginosa* of some of the nanocomposite samples are shown in Figure 11 and Table II. Samples of CP substrate with various silver nanoparticles contents were selected for antimicrobial analysis because they showed higher hydrogel/silver nanoparticles contents, and only a few C substrate samples (0.02 and 0.14*M*) were analyzed for comparative purposes. From the results, we determined that the samples of CHAg (with 0.14*M* silver) and all samples with CPHAg with silver contents higher than 0.06*M* were very effective biocides against this type of bacteria. It was possible to confirm that both substrate samples, C and CP, without silver did not show any inhibition against this microorganism; we observed complete growth of this bacteria all over of these substrates. On the other hand, samples with silver contents lower than 0.06*M* did not show an inhibitory effect against this type of bacteria.

The results for the samples tested against *S. aureus* are shown in Figure 12 and Table II. Inhibition zones could be observed for almost all of the silver-containing samples, except for the sample with the lower silver content (0.01*M*). Samples with higher silver contents presented a red inhibition zone, which was related to the catalytic activity of the silver that in contact with the bacteria may have colored the surrounded areas.[38]

The inhibition ratios for various samples against *P. aeruginosa* are shown in Table II. As shown in this table, the reference samples did not have antimicrobial activity. Inhibition rates higher than 90% were obtained for the 0.14*M* C samples and for the 0.06, 0.1, 0.14, 0.2 and 1*M* CP samples. The rest of the samples

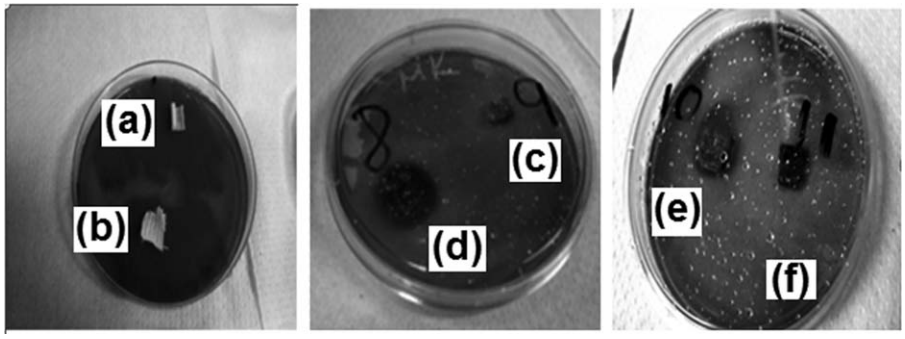

Figure 11. Photographic image of the incubation of the bacteria *P. aeruginosa* after 48 h on the reference samples: (a) C and (b) CP and CPHAg with (c) 0.1, (d) 0.14, (e) 0.2, and (f) 1.0*M* $AgNO_3$.

Table II. Inhibition Ratios against the Bacteria *P. aeruginosa* and *S. aureus* for Specified Samples

	P. aeruginosa		*S. aureus*	
Sample	CFU/mL	Inhibition ratio (%)	CFU/mL	Inhibition ratio (%)
C	2.63×10^7	0.00	2.19×10^7	0.00
CP	2.59×10^7	0.00	2.23×10^7	0.00
0.02*M* CHAg	2.48×10^7	5.70	2.01×10^7	8.22
0.14*M* CHAg	1.56×10^6	94.07	1.63×10^6	92.56
0.01*M* CPHAg	1.94×10^7	25.10	1.93×10^7	13.45
0.02*M* CPHAg	2.08×10^7	19.69	1.86×10^7	16.59
0.06*M* CPHAg	1.39×10^6	94.63	1.31×10^7	41.26
0.1*M* CPHAg	1.46×10^6	94.36	1.43×10^6	93.59
0.14*M* CPHAg	2.01×10^6	92.24	1.39×10^6	93.77
0.2*M* CPHAg	1.29×10^6	95.02	1.24×10^6	94.44
1.0*M* CPHAg	1.15×10^6	95.56	1.19×10^6	94.66

(with 0.01 and 0.02*M* concentrations) showed lower inhibition rates around 5–25%.

The observed difference in the antimicrobial effect between the C and CP substrates could be attributed to the final amount of hydrogel coating between both substrates, whereas the C textile substrate retained only 36.7 wt % of the hydrogel coating. The CP substrate had a hydrogel coating of 86.8 wt %. With higher hydrogel contents, an increased silver nanoparticle concentration could be obtained, and thus a higher antimicrobial effect was observed. This difference was more notorious at lower silver nanoparticle contents.

Silver nanoparticles immersed and dispersed in the hydrogel coating of the textile substrate were responsible for the antimicrobial effect of these samples. Different mechanisms of the actions of silver have been reported in the literature, but the actual mechanism is still under investigation. The most probable mechanism may be due to the presence of interactions of silver ions that interfere with the replication process and results in cell death. Other mechanisms involve the penetration of silver nanoparticles through the cell wall of the microorganisms and consequently turn the DNA into a condensed form, which reacts with the thiol group of proteins and results in cell death.[39]

This Table II also shows the inhibition ratio against *S. aureus*, in which the antimicrobial activity was similar to that obtained against *P. aeruginosa* bacteria. The main difference between the antimicrobial activities against these two types of bacteria was obtained for the CP sample with 0.06*M*, which presented only a 41.2% of inhibition against *S. aureus*; this was lower than that obtained for *P. aeruginosa*.

CONCLUSIONS

An AA/IA copolymer hydrogel was obtained via free-radical polymerization.

An adequate dispersion of silver nanoparticles generated *in situ* into the hydrogel coating was obtained with average size distributions below 100 nm.

It was demonstrated that the obtained hydrogel silver nanocomposite was adequate for coating the C and CP substrates.

The *in situ* preparation of silver nanoparticles was a suitable method for producing nanosilver particles in the hydrogel coating with good dispersion and distribution.

Inhibition rates against *P. aeruginosa* and *S. aureus* higher than 90% were obtained when we used $AgNO_3$ contents higher than 0.1*M*.

It was possible to obtain a textile substrate coated with a silver hydrogel nanocomposite with excellent antimicrobial properties that showed their potential to be used as antibacterial materials, such as in wounds covers, medical textiles, and gloves.

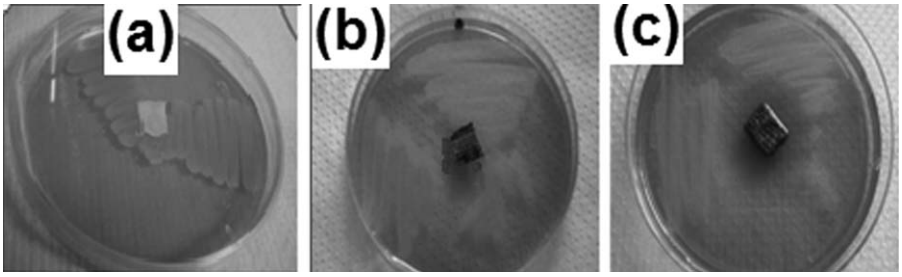

Figure 12. Photographic image of the incubation of the bacteria *S. aureus* after 48 h on the reference sample: (a) C and CPHAg with (b) 0.2 and (c) 1.0*M* $AgNO_3$.

ACKNOWLEDGMENTS

The authors gratefully acknowledge the financial support of Consejo Nacional de Ciencia y Tecnología through project: CB-104865. The authors would like to thank Araceli-Noxpanco, Alejandro-Espinoza, Marcelina-Sanchez, Jesus-Rodriguez, Fabian-Chavez, Francisco-Zendejo, M Lourdes-Guillen, Jose Lopez-Rivera, Patricia-Siller, Jesus-Cepeda Garza, Silvia-Torres, Maria Luisa-Lopez, Hugo Felipe-Jimenez and Miriam-Lozano for their technical support. They also would like to thank Paredes from UA de C for their appreciable collaboration in the antimicrobial tests.

REFERENCES

1. Sun, Y.; Sun, G. *J. Appl. Polym. Sci.* **2002**, *84*, 1592.
2. Kim, Y. H.; Sun, G. *Text. Res. J.* **2002**, *72*, 1052.
3. Wohrmann, R. M. J.; Hentschel, T.; Munstedt, H. *Adv. Eng. Mater.* **2000**, *2*, 380.
4. Zhu, P.; Sun, G. *J. Appl. Polym. Sci.* **2004**, *93*, 1037.
5. Freddi, G.; Arai, T.; Colonna, G. M.; Boschi, A.; Tsukada, M. *J. Appl. Polym. Sci.* **2001**, *82*, 3513.
6. Gupta, P.; Bajpai, M.; Bajpai, S. K. *J. Macromol. Sci. Pure Appl. Chem.* **2008**, *45*, 179.
7. Pal, S.; Tak, Y. K.; Song, J. M. *Appl. Environ. Microbiol.* **2007**, *73*, 1712.
8. Duran, N.; Marcato, P. D.; De Souza, G. I. H.; Alves, O. L.; Esposito, E.J. *Nanotechnol.* **2007**, *3*, 1.
9. Li, P.; Li, J.; Wu, C.; Wu, Q.; Li, J. *Nanotechnology.* **2005**, *16*, 1912.
10. Vegera, A. V.; Zimon, A. D. J. *Appl. Chem.* **2006**, *79*, 1403.
11. Martínez, N.; Niño, F.; Martínez, J. R.; Martínez, F.; Ruiz, M. J. *Nanopart. Res.* **2008**, *10*, 1343.
12. Song, K.; Lee, S.; Park, S. *Korean J. Chem. Eng.* **2009**, *26*, 153.
13. Falletta, E.; Bonini, M.; Fratini, E.; Lo Nostro, A.; Pesavento, G.; Becheri, A.; Lo Nostro, P.; Canton, P.; Baglioni, P. J. *Phys. Chem.* **2008**, *112*, 11758.
14. Zhang, J.; Wang, X.; Zhao, B.; Li, C. *Chem.Lett.* **2006**, *35*, 40.
15. Cabrera, J.; López, A.; Santiago, J. *Rev. Soc. Quím. Perú.* **2008**, *74*, 323.
16. Raffi, M.; Hussain, F.; Bhatti, T. M.; Akhter, J. I.; Hameed, A.; Hasan, M. M. *Mater. Sci. Technol.* **2008**, *24*, 192.
17. Furno, F.; Morley, K. S.; Wong, B.; Sharp, B. L.; Arnold, P. L.; Howdle, S. M.; Bayston, R.; Brown, P. D.; Winship, P. D.; Reid J. H. J. *Antimicrob. Chemother.* **2004**, *54*, 1019.
18. Gómez, J.; Aya Ramírez, O. *Rev. Colombiana Fís* **2009**, *41*, 385.
19. Yu, S. H.; Mi, F. L.; Wu, Y. B.; Peng, C. K.; Shyu, S. S.; Huang, R. N. J. *Appl. Polym. Sci.* **2005**, *98*, 538.
20. Mi, F. L.; Wu, Y. B.; Shyu, S. S.; Chao, A. C.; Lai, J. Y.; Su, C. C. J. *Membr. Sci.* **2003**, *212*, 237.
21. Seabra, A. B.; Oliveira, M. G. *Biomaterials* **2004**, *25*, 3773.
22. Cassu, S. N.; Felisberti, M. I. *Polymer* **1997**, *38*, 3907.
23. Nho, Y. C.; Park, K. R. J. *Appl. Polym. Sci.* **2002**, *85*, 1787.
24. Spanish Pat. ES 2,177,563 T3 (1994).
25. Varsha, T.; Namdeo, M.; Mohan, Y. M.; Bajpai, S. K.; Bajpai, M. J. *Macromol. Sci. Pure Appl. Chem.* **2008**, *45*, 107.
26. Dong, M.; Xie, X.; Zhang, L.-M. J. *Polym. Sci. Part B: Polym. Phys.* **2009**, *47*, 740.
27. Uygun, M.; Kahveci, M. U.; Odaci, D.; Timur, S.; Yagci, Y. *Macromol. Chem. Phys.* **2009**, *210*, 1867.
28. Tomic, S. L.; Dimitrijevic, S. I.; Marinkovic, A. D.; Najman. S. M.; Filipovic, J. M. *Polym. Bull.* **2009**, *63*, 837.
29. Carrillo, M.; Vivas, M.; Jiménez, L.; Hernández, L.; Ramírez, M.; Katime, I. *Rev. Iberoam. Polym.* **2009**, *10*, 188.
30. Mehlika Pulat, H. E. J. *Appl. Polym. Sci.* **2006**, *102*, 5994.
31. Wen-Fu, L.; Yu-Chen, H. J. *Appl. Polym. Sci.* **2007**, *106*, 1992.
32. Solomon, S.; Bahadory, M.; Jeyarajasingam, A.; Rutkowsky, S.; Boritz, C. J. *Chem. Educ.* **2007**, *84*, 322.
33. Lee, H.; Park, H.; Lee, H.; Kim, K.; Park, S. B. *Chem. Commun.* **2007**, *2959*.
34. Gupta, P.; Bajpai, M.; Bajpai, K. J. *Cotton Sci.* **2008**, *12*, 280.
35. Lee, H.; Yeo, S.; Jeong, S. J. *Mater. Sci.* **2003**, *38*, 2199.
36. Silvert, P.; Herrera-Urbina, R.; Duvauchelle, N.; Vijayakrishnan, V.; Elhsissen, K. T. J. *Mater. Chem.* **1996**, *6*, 573.
37. Murali Mohan, Y.; Mohana Raju, K.; Sambasivudu, K.; Singh, S.; Sreedhar, B. J. *Appl. Polym. Sci.* **2007**, *106*, 3375.
38. U.S. Pat. 2007/0003603 A1 (2007).
39. Dallas, P.; Sharma, V. K.; Zboril, R. *Adv. Colloid Interface Sci.* **2011**, *166*, 119.